Supporting information

Aqueous Ion Trapping and Transport in Graphene-embedded 18-crown-6 Ether Pores

Alex Smolyanitsky, Eugene Paulechka, Kenneth Kroenlein

S1. Ionic fluxes

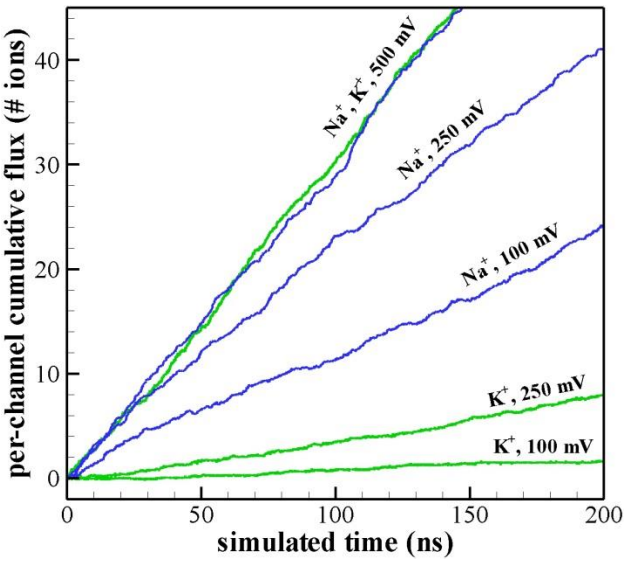

Figure S1. Typical cumulative fluxes obtained for different transmembrane voltages (0.5 M *KCl* and *NaCl*). Zero Cl^- fluxes were obtained in all simulations.

S2. Permeation and membrane potential in a 20-pore membrane

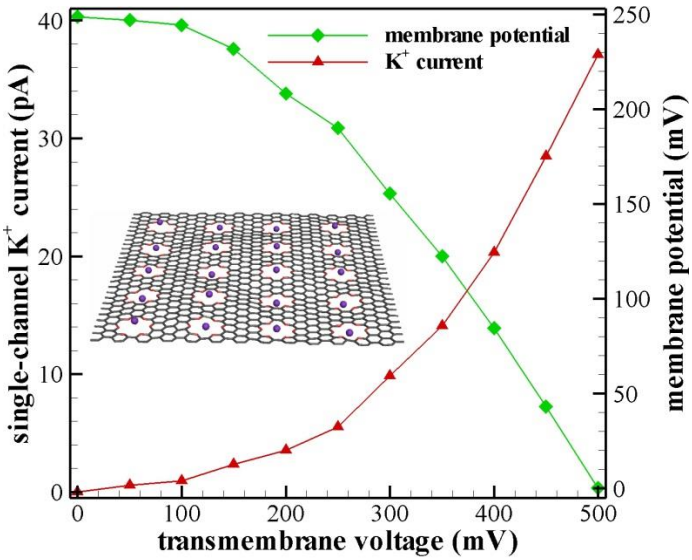

Figure S2. Simulated current and membrane potential as functions of the voltage across a 20-pore membrane (a fully occupied state is shown in the inset) for 0.5 M *KCl*. Each point was obtained from a 200 ns long room-temperature MD simulation, as described in the main text.

S3. Transistor sensitivity tuning

We rewrite Eq. (1) from the main text and replace the salt bulk concentration c with $c\exp\left(-\frac{qV_g}{k_bT}\right)$:

$$I = \frac{qk_dc\exp\left(-\frac{qV_g}{k_bT}\right)\sinh\left(\frac{qV}{2k_bT}\right)}{K_d\cosh\left(\frac{qV}{2k_bT}\right)+c\exp\left(-\frac{qV_g}{k_bT}\right)} \quad \text{(S1)}$$

The differential per-pore transconductance is

$$g(c) = \frac{dI}{dV_g} = -\frac{q^2k_dK_d}{k_bT}f_1(V)\,c\left(K_df_2(V) + c\exp\left(-\frac{qV_g}{k_bT}\right)\right)^{-2}, \quad \text{(S2)}$$

where $f_1(V) = \sinh\left(\frac{qV}{2k_bT}\right)\cosh\left(\frac{qV}{2k_bT}\right)$ and $f_2(V) = \cosh\left(\frac{qV}{2k_bT}\right)$. The absolute value of g is maximized at $K_df_2 = c\exp\left(-\frac{qV_g}{k_bT}\right)$, yielding

$$c_0 = K_d\exp\left(\frac{qV_g}{k_bT}\right)\cosh\left(\frac{qV}{2k_bT}\right). \quad \text{(S3)}$$

With k_d and K_d used in the main text, we can evaluate Eqs. (S2) and (S3) for *KCl*. At an operating point of V = 200 mV and the current modulated around $V_g = 0$, we obtain c_0= 0.26 M and $g(c_0) \approx$ -0.44 nS. At a higher operating point of V = 300 mV, c_0= 1.78 M and a considerably larger optimal transconductance is obtained: $g(c_0) \approx$ -3.0 nS. Presented calculations are only accurate at the order-of-magnitude level, but clearly demonstrate that transistor sensitivity exhibits resonant properties with respect to salt concentration, and is realistically tunable for a selected operating transmembrane voltage V. *KCl* concentration yielding maximal absolute value of transconductance as a function of V is shown in Fig. S2. The inset demonstrates resonant behavior of $|g|$ with respect to c at V = 200 mV.

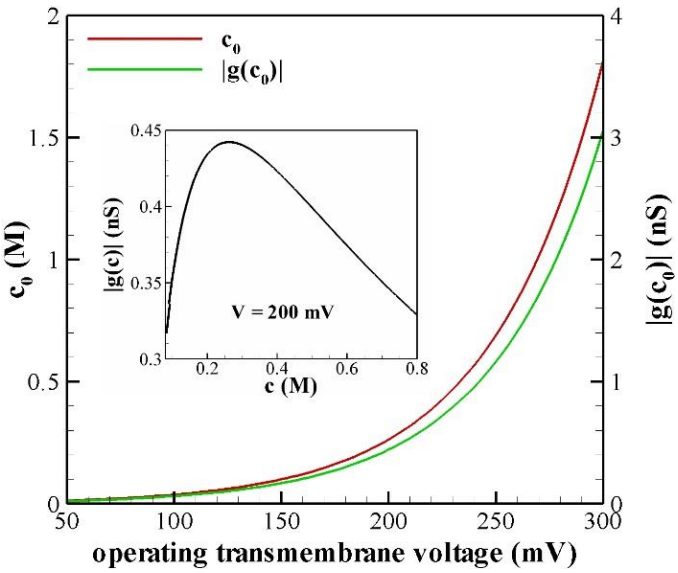

Figure S3. Optimal *KCl* concentration c_0 as a function of selected transmembrane voltage operating point around V_g = 0. The inset shows absolute value of transconductance $|g|$ as a function of bulk salt concentration for V = 200 mV with a maximum at c_0 = 0.26 M.

S4. Structure and atomic charges in graphene-embedded 18-crown-6 pores

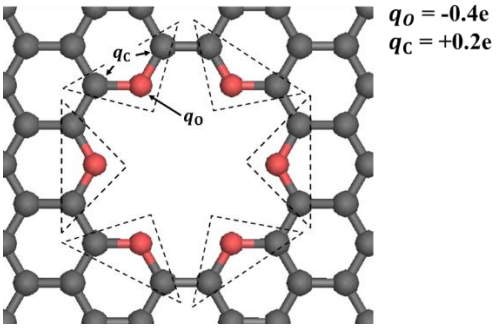

Figure S4. Atomic charges, according to the OPLS-AA forcefield; the circular charge distribution was confirmed by quantum-mechanical calculations. Each resulting dipole is outlined by a dashed triangle and the charges of each atomic species are equal between dipoles.

A direct replacement of sp^2 carbons with oxygens in an infinite pristine graphene sheet will necessarily introduce defects like uncompensated charge, or require extra hydrogenation to obtain system neutrality. However, in a finite sheet interfaced with a conducting substrate, however large, this situation can be avoided (see, for example, Fig. S5 with hydrogen-passivated edges).

A realistic graphene sample is expected to have naturally occurring defects, including C-H, C-O, or C=O bonds, which, along with the presence of mobile charge in graphene, can compensate for the defects from introducing the pore structure, thus maintaining electrical neutrality of the overall system. The correctness of this assumption is supported by Figure 2 of Ref. 6 in the main text, where most of the experimentally obtained oxygen-containing rings are shown to contain six atoms. As a result, a simplified model presented here should be able to describe the main features of the crown-porous membrane in terms of its interactions with aqueous ions. In addition, such a simplification is not expected to produce a noticeable effect on the parameters used in the MD simulations. At the same time, more rigorous calculations (for example, using density functional theory) require explicit consideration of the defects. All charges shown in Fig. S4, along with the planarity of the pore region, were confirmed by independent quantum-mechanical calculations (CHELPG scheme[1] at the *HF/6-31+G(d)* theory level, using Gaussian 09 software[2]) performed on a structure with defects similar to those shown in Fig. S5.

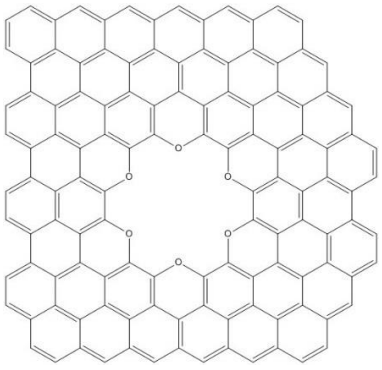

Figure S5. Bond distribution in a finite graphene sample with hydrogen-terminated edges and an embedded 18-crown-6 pore.

References

1. Breneman, C. M.; Wiberg, K. B., Determining Atom-Centered Monopoles from Molecular Electrostatic Potentials. The Need for High Sampling Density in Formamide Conformational Analysis. *J. Comput. Chem.* **1990,** *11*, 361-373.
2. Frisch, M. J.; Trucks, G. W.; Schlegel, H. B.; Scuseria, G. E.; Robb, M. A.; Cheeseman, J. R.; Scalmani, G.; Barone, V.; Mennucci, B.; Petersson, G. A.; Nakatsuji, H.; Caricato, M.; Li, X.; Hratchian, H. P.; Izmaylov, A. F.; Bloino, J.; Zheng, G.; Sonnenberg, J. L.; Hada, M.; Ehara, M., *et al. Gaussian 09*, Gaussian, Inc.: Wallingford, CT, USA, 2009.